applied sciences

MDPI

*Article*

# Exploring Generative Adversarial Network-Based Augmentation of Magnetic Resonance Brain Tumor Images

**Mahnoor Mahnoor, Oona Rainio and Riku Klén ***

Turku PET Centre, University of Turku, Turku University Hospital, FI-20014 Turku, Finland; mahnoor.m.mahnoor@utu.fi (M.M.); ormrai@utu.fi (O.R.)
* Correspondence: riku.klen@utu.fi

**Abstract:** Background: A generative adversarial network (GAN) has gained popularity as a data augmentation technique in the medical field due to its efficiency in creating synthetic data for different machine learning models. In particular, the earlier literature suggests that the classification accuracy of a convolutional neural network (CNN) used for detecting brain tumors in magnetic resonance imaging (MRI) images increases when GAN-generated images are included in the training data together with the original images. However, there is little research about how the exact number of GAN-generated images and their ratio to the original images affects the results obtained. Materials and methods: Here, by using 1000 original images from a public repository with MRI images of patients with or without brain tumors, we built a GAN model to create synthetic brain MRI images. A modified U-Net CNN is trained multiple times with different training datasets and its classification accuracy is evaluated from a separate test set of another 1000 images. The Mann–Whitney U test is used to estimate whether the differences in the accuracy caused by different choices of training data are statistically significant. Results: According to our results, the use of GAN augmentation only sometimes produces a significant improvement. For instance, the classification accuracy significantly increases when 250–750 GAN-generated images are added to 1000 original images ($p$-values $\leq 0.0025$) but decreases when 10 GAN-generated images are added to 500 original images ($p$-value: 0.03). Conclusions: Whenever GAN-based augmentation is used, the number of GAN-generated images should be carefully considered while accounting for the number of original images.

**Keywords:** brain tumor; convolutional neural network; generative adversarial network; magnetic resonance imaging



**Citation:** Mahnoor, M.; Rainio, O.; Klén, R. Exploring Generative Adversarial Network-Based Augmentation of Magnetic Resonance Brain Tumor Images. *Appl. Sci.* **2024**, *14*, 11822. https://doi.org/10.3390/app142411822

Academic Editors: Asiya Khan and Gloria Iyawa

Received: 4 November 2024
Revised: 5 December 2024
Accepted: 12 December 2024
Published: 18 December 2024



## 1. Introduction

A convolutional neural network (CNN) is a subtype of an artificial neural network specifically designed for processing image data. During the past decades, CNNs have become very popular in the medical field because they can be used to create automatic tools for helping physicians in many routine tasks, which are entailed in their work [1–3]. However, the CNNs require labeled image data for their training, and since the availability of the patient data is often limited due to privacy concerns, we often need augmentation in order to increase the amount of existing data.

The simplest types of augmentation are based on geometric transformations such as reflections, rotations, and translations. For instance, we can quadruple the number of images in the training data by first including all the vertical reflections of the original images and then the horizontal reflections of both the original images and their vertical reflections. Additionally, Möbius transformations or other conformal mappings can be used to create more complicated and diverse augmented images [4].

In 2014, Goodfellow et al. [5] introduced a generative adversarial network (GAN), a new type of neural network design capable of creating synthetic images that resemble the original training images. The structure of a GAN consists of two neural networks: the

generator and the discriminator. During the training process of a GAN, random input values from training data are given to the generator to create new data values through unsupervised learning, and the discriminator tries to distinguish images between the original images and the synthetic data produced by the generator. The GAN model is trained to the level where the generated data have the same characteristics as the training data. During the past decade, limited data on specific medical conditions, due to privacy and scarcity of disease occurrence, have motivated the generation of GAN-augmented data for supporting research work in the medical field. Nowadays, GAN is widely used in healthcare to generate medical images because of its robustness and efficiency.

## 2. Related Work

Multiple different GAN models have been used to augment data related to various diseases across the subfields of medicine. For instance, Xing et al. [6] proposed the use of GANs to improve disease localization in pulmonary pathology. Lin et al. [7] suggested that GANs could be used to address the issue of data scarcity in mammography and trained for the mass detection of breast cancer. Additionally, Chen and Cao [8] concluded that with a small dataset related to diabetic neuropathy, GAN has a more significant effect on data augmentation than traditional augmentation.

In neuro-oncology, several GAN models have been introduced to improve brain tumor classification. S. Deepak et al. used a GAN-based augmentation of multi-class brain tumor classification from magnetic resonance imaging (MRI) scans and synthesized data for meningioma, glioma, and pituitary tumor [9]. The tumor was classified by designing a deep CNN model. A similar GAN was introduced by Biswas et al. [10]. Their study used a three-dimensional (3D) U-net GAN architect to augment the images, and a random forest classifier was used for classification. Liu et al. [11] introduced another GAN for the creation of MRI brain fusion images with detailed contrast information of brain tumor tissues of multi-modal MRI images. The generator model of GAN in their study was a nested U-net structure with residual U-shaped blocks. The proposed model outperformed many common fusion techniques according to qualitative metrics. Similarly, Ge et al. [12] also studied GANs for brain tumor classification in multimodality MRI images.

However, in many earlier studies (e.g., [6,7,12,13]), the impact of GAN-based augmentation has been confirmed only for specific choices of the numbers of the original images and the GAN-generated images. For instance, Ge et al. [12] reported that adding 198 GAN-generated images to the training data of 792 original images increased the accuracy of a CNN-based classifier from 78.46% to 81.03% but did not repeat this experiment with different choices for numbers of images. Consequently, this raises a question about how sensitive the benefit gained from the GANs is to the exact number of GAN-generated used and their ratio to the original images. Therefore, an appropriate GAN model tested with a different number of training datasets is essential to find out how the number of GAN-generated images affects the performance of the binary classifier.

In our paper, we evaluate the impact of including synthetic images created by a GAN in the training data of a CNN on its accuracy in classifying brain MRI images based on whether the patient has a brain tumor or not. We build a deep convolutional GAN (DCGAN) for creating synthetic images and a modified U-Net CNN for image classification. We use statistical testing to assess whether the observed differences in the accuracy of the classification CNN trained with training datasets are statistically significant or not.

## 3. Materials and Methods

### 3.1. Software Requirements

The experiments were run on Python [14] (version: 3.9.9) by using packages Keras [15] (version: 2.15.0) and Tensorflow [16] (version: 2.15.0). The supercomputer Puhti (version: 3.1.7) at CSC-IT Centre for Science Ltd. [17] was used for computational resources.

### 3.2. Data and Pre-Processing

We used 2000 transaxial two-dimensional brain MRI images with and without brain tumors from the publicly available dataset Br35h:: Brain Tumor Detection 2020 [18]. Out of these 2000 original images, 1000 images were positive for brain tumors, and 1000 images were negative for brain tumors (healthy controls). The images were cropped to remove the empty background with an algorithm that chose the largest rectangle with non-empty borders within the original images. All the images were then converted into the size of $64 \times 64$ pixels, and they were already originally grayscale.

### 3.3. GAN for Augmentation

Our GAN design is a DC-GAN, originally introduced by Radford et al. [19] in 2015 and built by using the code in [18]. Like all GANs, our design has a generator and a discriminator. Our model requires the machine learning libraries: TensorFlow and Keras. The dataset is first resized to $64 \times 64$ and then loaded in the model for processing. The generator model architecture is made in a way that creates images, while the discriminator architecture functions to differentiate between generated and real images.

The main layers used to create a generator are dense, LeakyReLU activation, Reshape, and transposed convolutional layers. The generator starts with the dense layer with $8 \times 8 \times 512$ neurons, followed by LeakyReLU activation. These neurons are upsampled through 4 transposed convolutional layers with filters added. Filters are progressively decreasing as 256, 128, and 64, each filter followed by LeakyReLU except for the last layer, which uses the hyperbolic tangent function tanh. Here, the number of color channels was set to 1 as we generated greyscale images. The model is compiled by binary cross entropy and optimized by Adam optimizer.

The discriminator takes an input image size of $64 \times 64 \times 1$, which is either a real image from the original dataset or generated images from the generator model. The discriminator model consists of 4 convolutional layers with increasing filters, 64, 128, 128, and 256, and the kernel used in convolutional layers is $3 \times 3$. The convolutional layers progressively downsamples the image while increasing the depth of feature maps. All layers are followed by the LeakyReLU activation function, which adds non-linearity to the code and helps understand complex data. After these convolutional layers, the image is flattened into a 1D vector, and a dropout and dense layer is applied. The dropout layer prevents overfitting by deactivating a fraction of neurons with a dropout rate of 0.4. The dense layer with a single neuron and sigmoid activation is added to the discriminator to indicate whether an image is real or fake. The main idea was to use transposed convolutional layers in the generator and the convolutional layers in the discriminator. The model is compiled by binary cross entropy and optimized by Adam optimizer. A function called 'sample_images' is called to generate images from the noise input using GAN generator architecture. Table 1 refers to the hyperparameters used in the code with actual numbers representing how the network is trained.

**Table 1.** Hyperparameters used in the Generative Adversarial Network code for generating augmented data.

| Hyperparameters | GAN Model |
|---|---|
| Noise Dimension | 100 |
| Batch size | 4 |
| Epochs | 100 |
| Steps per epoch | 3750 |
| Learning Rate | 0.0002 |
| Decay Factor | 0.5 |
| Image Dimension of training data | $64 \times 64$ |
| Channels | 1 |
| Dropout rate for discriminator | 0.4 |

The original code is available at https://github.com/rklen/GAN_for_brain_tumor_MRIs/tree/main (accessed on 23 August 2024).

### 3.4. CNN for Classification

U-Net, originally for medical image segmentation introduced by Ronneberger et al. [20], is a lightweight CNN architecture consisting of two paths, the first of which decreases the image dimensions and the latter of which enlarges the dimensions back to the original. In this way, U-Net can first see the whole image at once to understand its context and then focus on the details required for accurate segmentation. However, in research by Hellström et al. [21], it was noted that the sole constricting path of a typical U-Net can be used to create an efficient CNN for classifying medical images based on the presence of cancer. Here, we use the modified U-Net from [21]: The CNN contains four sequences of two convolutional layers and one maximum pooling layer, followed by four dense layers. We use stochastic gradient descent as an optimizer with a learning rate of 0.001 and binary entropy as a loss function. During the training, 30% of the training data are used for validation, ensuring that the model is training on a separate set of validation during training to detect overfitting. The number of epochs was set to 100.

### 3.5. Data Division and Training of the Models

Figure 1 explains the dataset division. The dataset was divided into an equal number of training and testing datasets. Both datasets have an equal number of tumor-positive and tumor-negative images. The GAN was trained twice with the training dataset, first on 500 positive and then on 500 negative original images from the training dataset, and the model synthesized 500 positive and 500 negative augmented images. In sum, we generated 1000 synthetic images. Each image was generated based on 100 epochs after ten iterations. The image from 1 to 100 epochs generated from the 1000 training dataset is mentioned in Figure 2. The final GAN-generated images were $64 \times 64$ pixels in grayscale as the original images.

The training dataset of the classifier CNN was always a combination of the same original images that were used to train the GAN and some number of synthetic GAN-generated images. The number of positive and negative images was always equal within both the original images and the GAN-generated images in each training set. For each training set used, we re-initialized and trained the CNN 20 times to decrease the impact of random variation from our results. After each training iteration, the CNN was used to predict a separate test set containing the remaining 500 brain tumor-positive and 500 healthy controls excluded both from the training of the GAN and the classifier CNN.

### 3.6. Evaluation and Statistical Testing

The classification results of the CNN were evaluated in terms of accuracy (ratio between the numbers of correctly classified instances and all the instances) after each 20 iterations. We use Youden's threshold based on the predictions of the training data of each specified set of images to convert the numerical predictions into binary labels. We then computed the mean and the standard deviation of the classification accuracy of the test set over these 20 iterations. To compare the values of accuracy obtained with training datasets with and without GAN-generated images, we use the Mann–Whitney U test [22]. The Mann–Whitney U test is a statistical nonparametric text for the null hypothesis [23]. This test was conducted between the accuracy values of the test set predictions by the CNN, whose training data contain both original and GAN-generated images, and the corresponding accuracy obtained without using any GAN-generated images. Our null hypothesis was that the use of GAN-generated images in the training did not cause significant differences in the accuracy. We use the typical level of significance of 5% but take the multiple comparisons problem into account before drawing final conclusions.

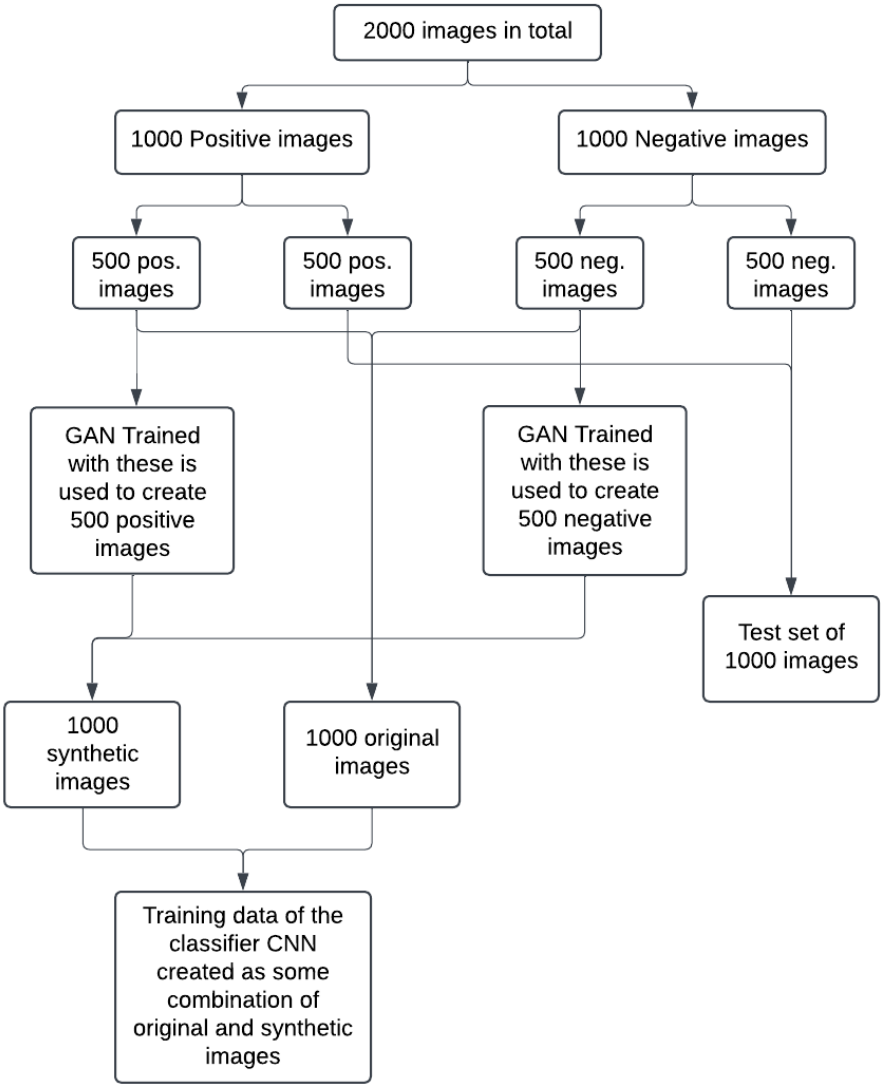


**Figure 1.** A graph explaining the dataset division.

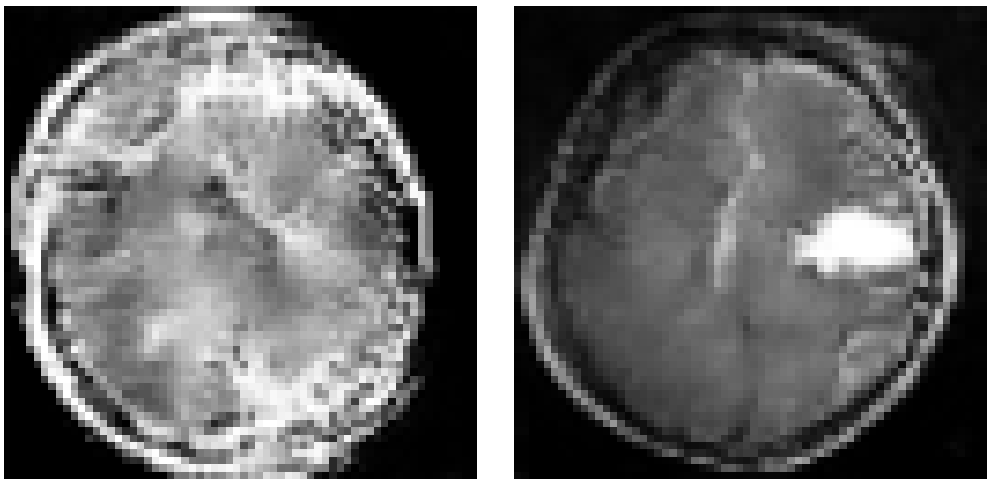

(**a**) (**b**)

**Figure 2.** GAN output using 1000 training datasets at the following epochs: (**a**) 1 epoch; (**b**) 100 epochs.

## 4. Results

Our results are summarized in Tables 2 and 3, and Figure 3 also shows examples from training data and GAN-generated images. Table 2 contains the mean values of the 20 accuracy values computed from original and GAN-generated images when either no GAN-generated images or up to 1000 GAN-generated images. The results show a maximum mean accuracy of 88% with a 3% standard deviation when 1000 original images and 500 GAN-generated images were tested.

Table 3 tells us about the significant difference between original and GAN-generated images using the Mann–Whitney U-test. According to Table 3, there are statistically significant differences between the datasets when 250, 500, and 750 GAN-generated images are added with training data of 50, 500, and 1000 original images. Comparing this to Table 2, we see that the highest values of accuracy are obtained with 250, 500, and 750 GAN-generated images with 1000 original images, so the use of GAN augmentation also significantly increased the accuracy in these cases. However, adding more GAN data was not always helpful, and, in particular, adding 10 GAN-generated images to 500 original images significantly decreased the accuracy.

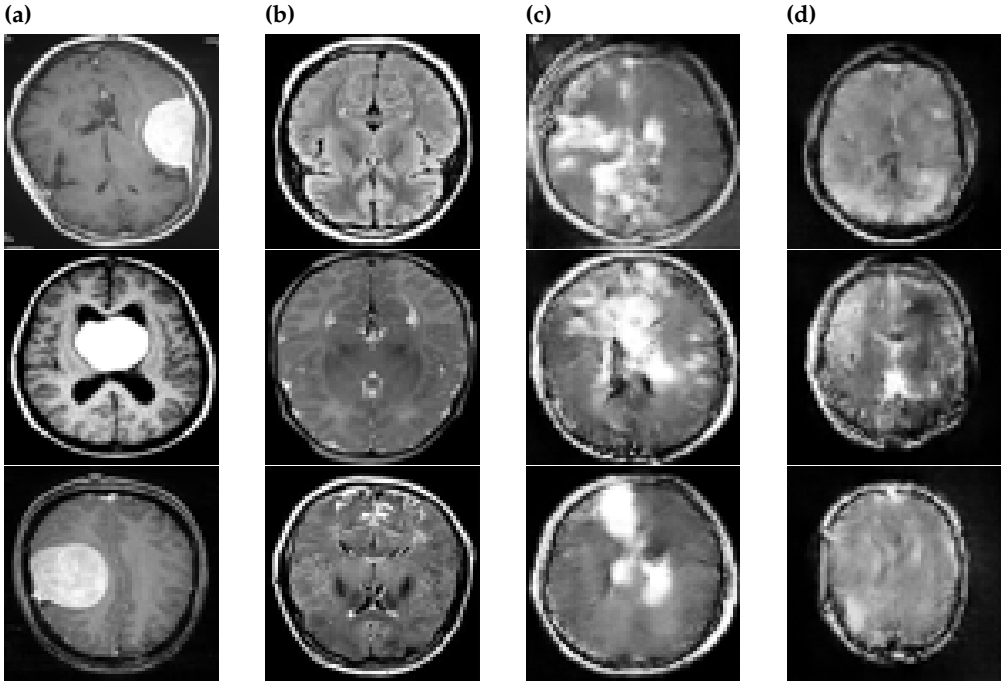


**Figure 3.** Examples of the following are given: (**a**) Positive images in the original dataset; (**b**) Negative images in the original dataset; (**c**) Positive images created by GAN; (**d**) Negative images created by GAN.

**Table 2.** Mean ± standard deviation values for the accuracy over 20 iteration rounds when the CNN is trained by using a dataset consisting of the specified numbers of original images and synthetic images created by the GAN. The values in bold are related to the *p*-values of Table 3.

| | | **Original Images** | | | |
|---|---|---|---|---|---|
| | | **12** | **50** | **500** | **1000** |
| GAN images | 0 | 0.60 ± 0.07 | 0.56 ± 0.06 | 0.77 ± 0.03 | 0.82 ± 0.05 |
| | 10 | 0.61 ± 0.05 | 0.56 ± 0.06 | 0.75 ± 0.03 | 0.83 ± 0.05 |
| | 50 | 0.57 ± 0.06 | 0.55 ± 0.06 | 0.77 ± 0.02 | 0.82 ± 0.04 |
| | 250 | 0.61 ± 0.04 | 0.52 ± 0.07 | 0.76 ± 0.03 | **0.87 ± 0.02** |
| | 500 | 0.63 ± 0.04 | 0.60 ± 0.04 | 0.76 ± 0.03 | **0.88 ± 0.03** |
| | 750 | 0.62 ± 0.03 | 0.54 ± 0.08 | 0.76 ± 0.03 | **0.87 ± 0.02** |
| | 1000 | 0.59 ± 0.07 | 0.57 ± 0.04 | 0.75 ± 0.03 | 0.85 ± 0.04 |

**Table 3.** The *p*-values of Mann–Whitney U test comparing the classification accuracies of the CNNs trained with training data containing both the specified numbers of original images and synthetic GAN images with the CNN trained with same number of original images but no GAN images.

| | | **Original Images** | | | |
|---|---|---|---|---|---|
| | | **10** | **50** | **500** | **1000** |
| GAN images | 10 | 0.86 | 0.80 | **0.03** | 0.70 |
| | 50 | 0.18 | 0.55 | 0.59 | 0.51 |
| | 250 | 1.00 | 0.10 | 0.08 | **0.00023** |
| | 500 | 0.12 | **0.01** | 0.21 | $\mathbf{3.7 \times 10^{-5}}$ |
| | 750 | 0.55 | 0.52 | 0.21 | **0.0025** |
| | 1000 | 0.76 | 0.77 | 0.10 | 0.09 |

## 5. Discussion

Our results show that the effect of adding GAN-generated synthetic images to training data on accuracy strongly depends on both the number of original images and the number of synthetic images to be added. For instance, adding 250–750 GAN-generated images to the training data of 1000 images significantly increased the classification accuracy of the modified U-Net ($p$-values $\leq 0.0025$). Still, using GAN-generated images did not often produce any statistical significance, and adding 10 GAN-generated images to 500 original images significantly decreased the classification accuracy ($p$-value: 0.03). While this is partially caused by the multiple comparisons problem, as repeating a statistical test several times increases the likelihood of incorrectly rejecting a true null hypothesis, our results still suggest that the number of GAN-generated images and, in particular, their ratio with the original images should be considered carefully.

We expected the 1000 GAN-generated images to give a high mean accuracy and be statistically significantly different from the original images. Still, they could have performed better compared to 250, 500, and 750 GAN-generated images. The maximum mean accuracy of 88% was achieved with 500 GAN-generated images. However, the model performed well when the dataset contained less than 500 GAN images against a certain number of original images.

This model is adaptive to publicly available data and tested on random MRI images. The model has yet to be tested on specifications like T1, T2, Flair, Contrast, and functional MRI or scans with different magnetic field strengths. Likewise, the model has yet to be tested on different image dimensions (i.e., $512 \times 512$, $1024 \times 1024$ pixel image). However, the framework can be adjusted according to the dataset's specifications to improve the model's performance and accuracy. This model generates images with the real-world benefit of using them as oversampling for research purposes.

## 6. Conclusions

This paper uses a GAN-based augmentation method to address the shortage of transaxial brain MRI images with tumors. The model generated $64 \times 64$ realistic brain MRI images and performed well in tumor detection. The images were verified by testing them multiple times with U-Net CNN classification. By increasing the number of added GAN-generated images in the classifier, the U-Net CNN improved the mean accuracy from $82 \pm 5\%$ to $88 \pm 3\%$. The results prove that the proposed GAN model can generate images for imaging modalities other than MRI.

Future work should include extending this research to 3D medical images. Furthermore, extending this work to explore other GAN application techniques like Cycle GAN and comparing these two models should be performed to find the difference between the two and the best working model for real-world advantage. Also, the work should be extended to other imaging modalities.

**Author Contributions:** Conceptualization, M.M. and O.R.; methodology, M.M. and O.R.; validation, M.M., O.R. and R.K.; formal analysis, M.M.; investigation, M.M.; data curation, M.M. and O.R.;

writing—original draft preparation, M.M. and O.R.; writing—review and editing, O.R. and R.K.; visualization, R.K.; supervision, R.K.; project administration, O.R. and R.K. All authors have read and agreed to the published version of the manuscript.

**Funding:** The first author was funded by Finnish State Research Funding, and the second author was funded by the Finnish Culture Foundation and Sakari Alhopuro Foundation.

**Institutional Review Board Statement:** Not applicable.

**Informed Consent Statement:** Not applicable, we used data from an already existing public repository.

**Data Availability Statement:** Available as a public repository on Github: https://github.com/rklen/GAN_for_brain_tumor_MRIs/tree/main (accessed on 23 August 2024). We used the publicly available dataset Br35h:: Brain Tumor Detection 2020 [18] https://www.kaggle.com/ahmedhamada0/brain-tumor-detection (accessed on 3 June 2024).

**Conflicts of Interest:** On behalf of all the authors, the corresponding author states that there are no conflicts of interest.

## References

1. Abdou, M.A. Literature review: Efficient deep neural networks techniques for medical image analysis. *Neural Comput. Appl.* **2022**, *34*, 5791–5812 [CrossRef]
2. Anwar, S.M.; Majid, M.; Qayyum, A.; Awais, M.; Alnowami, M.; Khan, M.K. Medical image analysis using convolutional neural networks: A review. *J. Med. Syst.* **2018**, *42*, 226. [CrossRef]
3. Kshatri, S.S.; Singh, D. Convolutional Neural Network in Medical Image Analysis: A Review. *Arch. Comput. Methods Eng.* **2023**, *30*, 2793–2810. [CrossRef]
4. Zhou, S.; Zhang, J.; Jiang, H.; Lundh, T.; Ng, A.Y. Data augmentation with Mobius transformations. *Mach. Learn. Sci. Technol.* **2021**, *2*, 025016. [CrossRef]
5. Goodfellow, I.; Pouget-Abadie, J.; Mirza, M.; Xu, B.; Warde-Farley, D.; Ozair, S.; Courville, A.; Bengio, Y. Generative adversarial nets. *Adv. Neural Inf. Process. Syst.* **2014**, *27*, 139–144.
6. Xing, Y.; Ge, Z.; Zeng, R.; Mahapatra, D.; Seah, J.; Law, M.; Drummond, T. Adversarial pulmonary pathology translation for pairwise chest X-ray data augmentation. In Proceedings of the Medical Image Computing and Computer Assisted Intervention–MICCAI 2019: 22nd International Conference, Shenzhen, China, 13–17 October 2019; Proceedings; Springer International Publishing: Berlin/Heidelberg, Germany, 2019; Part VI 22, pp. 757–765.
7. Lin, C.; Tang, R.; Lin, D.D.; Liu, L.; Lu, J.; Chen, Y.; Gao, D.; Zhou, J. Breast mass detection in mammograms via blending adversarial learning. In Proceedings of the Simulation and Synthesis in Medical Imaging: 4th International Workshop, SASHIMI 2019, Held in Conjunction with MICCAI 2019, Shenzhen, China, 13 October 2019; Proceedings 4; Springer International Publishing: Berlin/Heidelberg, Germany, 2019; pp. 52–61.
8. Chen, H.; Cao, P. Deep learning based data augmentation and classification for limited medical data learning. In Proceedings of the 2019 IEEE International Conference on Power, Intelligent Computing and Systems (ICPICS), Shenyang, China, 12–14 July 2019; pp. 300–303.
9. Deepak, S.; Ameer, P.M. MSG-GAN based synthesis of brain MRI with meningioma for data augmentation. In Proceedings of the 2020 IEEE International Conference on Electronics, Computing and Communication Technologies (CONECCT), Bangalore, India, 2–4 July 2020.
10. Biswas, A.; Bhattacharya, P.; Maity, S.P.; Banik, R. Data augmentation for improved brain tumor segmentation. *IETE J. Res.* **2023**, *69*, 2772–2782. [CrossRef]
11. Liu, X.; Chen, H.; Yao, C.; Xiang, R.; Zhou, K.; Du, P.; Liu, W.; Liu, J.; Yu, Z. BTMF-GAN: A multi-modal MRI fusion generative adversarial network for brain tumors. *Comput. Biol. Med.* **2023**, *157*, 106769. [CrossRef]
12. Ge, C.; Gu, I.Y.H.; Jakola, A.S.; Yang, J. Cross-modality augmentation of brain MR images using a novel pairwise generative adversarial network for enhanced glioma classification. In Proceedings of the 2019 IEEE International Conference on Image Processing (ICIP), Taipei, Taiwan, 22–25 September 2019; pp. 559–563.
13. Ghassemi, N.; Shoeibi, A.; Rouhani, M. Deep neural network with generative adversarial networks pre-training for brain tumor classification based on MR images. *Biomed. Signal Process. Control* **2020**, *57*, 101678. [CrossRef]
14. van Rossum, G.; Drake, F.L. *Python 3 Reference Manual*; CreateSpace: Scotts Valley, CA, USA, 2009.
15. Keras. GitHub, GitHub Repository. 2015. Available online: https://keras.io/about/ (accessed on 14 April 2024)
16. Abadi, M.; Agarwal, A.; Barham, P.; Brevdo, E.; Chen, Z.; Citro, C.; Corrado, G.S.; Davis, A.; Dean, J.; Devin, M.; et al. TensorFlow: Large-Scale Machine Learning on Heterogeneous Systems. 2015. Available online: https://www.tensorflow.org/ (accessed on 14 April 2024)
17. CSC—IT Center for Science, Finland. Available online: www.csc.fi (accessed on 3 June 2024).
18. Hamada, A. Br35h:: Brain Tumor Detection 2020, Version 12. Available online: https://www.kaggle.com/ahmedhamada0/brain-tumor-detection (accessed on 24 February 2023).

19. Radford, A.; Metz, L.; Chintala, S. Unsupervised representation learning with deep convolutional generative adversarial networks. *arXiv* **2015**, arXiv:1511.06434.
20. Ronneberger, O.; Fischer, P.; Brox, T. U-Net: Convolutional Networks for Biomedical Image Segmentation. In *Medical Image Computing and Computer-Assisted Intervention–MICCAI 2015. MICCAI 2015*; Navab N., Hornegger J., Wells W., Frangi A., Eds.; Lecture Notes in Computer Science; Springer: Cham, Switzerland, 2015; Volume 9351, pp. 234–241. [CrossRef]
21. Hellström, H.; Liedes, J.; Rainio, O.; Malaspina, S.; Kemppainen, J.; Klén, R. Classification of head and neck cancer from PET images using convolutional neural networks. *Sci. Rep.* **2023**, *13*, 10528. [CrossRef] [PubMed]
22. Riina, M.D.; Stambaugh, C.; Stambaugh, N.; Huber, K.E. Continuous variable analyses: T-test, Mann–Whitney, Wilcoxin rank. In *Translational Radiation Oncology*; Academic Press: Cambridge, MA, USA, 2023; pp. 153–163.
23. Călin, M.F.; Tuşa, E. Using t-Student and U-Mann-Whitney tests to identify differences in the study of the impact of the COVID-19 pandemic in online education in schools. Analele ştiinţifice ale Universităţii "Ovidius" Constanţa. *Ser. Mat.* **2023**, *31*, 39–59.